

# $H_\infty$ Weighted Integral Event-Triggered Synchronization of Neural Networks With Mixed Delays

Shen Yan , Sing Kiong Nguang , *Senior Member, IEEE*, and Zhou Gu

**Abstract**—This article considers an event-triggered  $H_\infty$  synchronization of neural networks (NNs) with mixed (discrete and distributed) delays. To release the communication burden, a novel weighted integral event-triggered scheme (IETS) is proposed based on the past information of the system dynamics. In this scheme, for the first time, a weighting function is proposed to weight the system state over a given period, which can be viewed as a forgetting factor. Moreover, a waiting time interval is added in the proposed IETS to exclude Zeno phenomenon. By constructing a novel Lyapunov–Krasovskii functional with the distributed delay kernel and the weighting function, sufficient linear matrix inequality conditions for the existence of an event-triggered controller that guarantees an exponential synchronization of the delayed NNs with an  $H_\infty$  performance are derived. Finally, an illustrative example and an application to image encryption are used to demonstrate the advantage of the proposed approach.

**Index Terms**—Distributed delay system, event-triggered control, neural networks, synchronization, weighting function.

## I. INTRODUCTION

NEURAL networks (NNs) have been proved to be effective for resolving complicated issues, such as control problem of grid integrated solar photovoltaic systems [1], [2] and artificial intelligence-based anomaly detection in cellular networks [3]. Recently, the synchronization of NNs has become an interesting topic due to its wide applications in image encryption [4], [5], secure communication [6], and so on. The aim of synchronization is using a controller to drive a slave system to track a master system. Over the past decade, various methods have

Manuscript received January 9, 2020; revised March 26, 2020 and May 15, 2020; accepted June 6, 2020. Date of publication June 23, 2020; date of current version January 4, 2021. This work was supported by National Natural Science Foundation of China under Grant 61473156 and Grant 61773200. Paper no. TII-20-0112. (*Corresponding author: Zhou Gu.*)

Shen Yan and Zhou Gu are with the College of Mechanical and Electronic Engineering, Nanjing Forestry University, Nanjing 210037, China (e-mail: yanshenzdh@gmail.com; gzh1808@163.com).

Sing Kiong Nguang is with the Department of Electrical Computer and Software Engineering, University of Auckland, Auckland 1142, New Zealand (e-mail: sk.nguang@auckland.ac.nz).

Color versions of one or more of the figures in this article are available online at <https://ieeexplore.ieee.org>.

Digital Object Identifier 10.1109/TII.2020.3004461

been adopted to deal with synchronization of NNs and chaotic systems, see [7], [8], and the references therein. In [9], a state feedback controller design is studied for synchronization of chaotic NNs with mixed delays. In [10], considering uncertain NNs with mixed delays, a synchronization controller is designed for both norm-bounded and polytopic uncertainties.

On the other research line, event-triggered scheme (ETS) has attracted many interests and attention due to its advantage of saving limited communication bandwidth of networked systems [11]–[16]. Consequently, much attention has been paid to improving the effectiveness of the triggering schemes. In [17], a dynamic ETS is presented to ensure the stability of linear systems via introducing an extra internal dynamic variable, where the Lyapunov function is not required to decrease monotonically. The fewer event triggers are obtained in [17] over the normal ETS in [18]. However, in these results, the controller is given in advance, which is independent of the event-triggered mechanism. To codesign the triggering parameters and controller gain simultaneously, a delay system approach is proposed in [19], which also has been applied in stabilization and synchronization of NNs [20]–[22]. To be specific, the synchronization problem of switched delayed NNs with event-triggered communication scheme is studied in [20]. The issue of the global synchronization of delayed memristive NNs is developed in [21], which needs the complex computation of the lower bound of two adjacent events to avoid Zeno behavior. To get rid of such complex computation burden, a switched ETS, switching between a waiting time interval and continuous triggering condition [24] is exploited to achieve exponential synchronization of delayed NNs with an extended dissipativity performance in [22]. In these results, only the instant state of system is used to design the triggering conditions. In real environments, however, the state of system could contain some random fluctuations caused by exogenous disturbance or environment noises. The state of system with such random fluctuations may be sensitive to the execution of the triggering rule, which may produce some unnecessary triggers. Therefore, IETSSs with an average value of the state of system are proposed in [25] and [26], which may be helpful in reducing the negative effect of random fluctuations. Specifically, [25] investigates an integral-based event-triggered control of linear time-invariant systems to attenuate the effect on system performance induced by measurement noise. In [26], for an unmanned surface vehicle with disturbance and failures, a fault detection

filter is designed under IETS, where network resources are saved significantly. It is noted that no weighting function is applied to weight the state of systems in [25] and [26]. Actually, the weighting coefficients of system states at different time instants can be different. Thus, it is more practical and reasonable to study the weighted IETS than the IETSs without weighting function. To our best knowledge, no research has been conducted on studying the integral-based event-triggered synchronization of delayed NNs, where the integral-based triggering condition is designed by using the weighted mean of system state.

Inspired by the above observations, this article investigates the synchronization of NNs with mixed delays via a weighted IETS. The effectiveness of the weighted event-triggered synchronization is illustrated via a numerical example. Its application to image encryption is presented in Section V, where the security of the proposed encryption algorithm against the differential attack is analyzed. The main contributions are summarized as follows.

1) A novel integral-based triggering rule based on a weighting function to weight the state of system over a period time is proposed. With the introduction of the weighting function, different weight of the past state of system can be adopted. The proposed weighted IETS is more general than the IETSs considered in [25] and [26], in which the weighting function can be viewed as a constant.

2) By integrating the weighted IETS, the event-triggered synchronization error system is formulated as a switched distributed delay system for excluding Zeno phenomenon. A new augmented Lyapunov–Krasovskii functional (LKF) related to the kernel of distributed delay of NNs and the weighting function of IETS is constructed. With the help of the integral inequality derived in [28], sufficient conditions for designing an event-triggered synchronization controller are given in terms of LMIs. This controller guarantees the synchronization of NNs with a required  $H_\infty$  performance.

Notation: In this article,  $\mathbb{R}^n$  is the Euclidean space with  $n$  dimension and  $\mathbb{R}^{n \times m}$  is used to represent the set of  $n \times m$  real matrices, respectively.  $\text{He}(P) = P^T + P$ . A symmetric and positive (negative) definite matrix  $P$  is denoted by  $P > 0$  ( $< 0$ ).  $*$  means  $[*]UV = V^TUV$  or  $V^T U[*] = V^TUV$ .  $\mathcal{L}_2[0, \infty)$  denotes the space of square-integrable vectors over  $[0, \infty)$ .  $\otimes$  means the Kronecker product. Matrices and vectors, if not explicitly stated, are assumed to be compatible for algebraic operations.

## II. PRELIMINARIES

Consider the following master–slave delayed NNs

$$\begin{cases} \dot{y}(t) = -Ay(t) + W_0\phi(y(t)) \\ \quad + W_1\phi(y(t-d)) + W_2 \int_{-d}^0 m(v)\phi(y(t+v))dv \\ \bar{z}(t) = Cy(t) \end{cases} \quad (1)$$

and

$$\begin{cases} \dot{\hat{y}}(t) = -A\hat{y}(t) + u(t) + D\omega(t) + W_0\phi(\hat{y}(t)) \\ \quad + W_1\phi(\hat{y}(t-d)) + W_2 \int_{-d}^0 m(v)\phi(\hat{y}(t+v))dv \\ \hat{z}(t) = C\hat{y}(t) + E\omega(t) \end{cases} \quad (2)$$

where  $y(t) = [y_1^T(t) y_2^T(t) \cdots y_n^T(t)]^T \in \mathbb{R}^n$  is the master system state,  $\hat{y}(t) = [\hat{y}_1^T(t) \hat{y}_2^T(t) \cdots \hat{y}_n^T(t)]^T \in \mathbb{R}^n$  is the slave system state,  $u(t) \in \mathbb{R}^n$  means the control input,  $\bar{z}(t) \in \mathbb{R}^p$  is the performance output of master system and  $\hat{z}(t) \in \mathbb{R}^p$  of slave system,  $m(v) \in \mathbb{R}$  is a continuous function meaning the distributed delay kernel,  $\omega(t) \in \mathbb{R}^r$  is the exogenous disturbance satisfying  $\mathcal{L}_2[0, \infty)$ ,  $\phi(y(t)) = [\phi_1(y_1(t)) \phi_2(y_2(t)) \cdots \phi_n(y_n(t))]^T \in \mathbb{R}^n$  denotes the neuron activation function, the constant scalar  $d$  means the discrete and distributed delays,  $A = \text{diag}\{a_1, \dots, a_n\}$  is a diagonal matrix with positive entries  $a_i > 0$ ,  $W_0 \in \mathbb{R}^{n \times n}$ ,  $W_1 \in \mathbb{R}^{n \times n}$  and  $W_2 \in \mathbb{R}^{n \times n}$  represent the connection weight matrices,  $E \in \mathbb{R}^{p \times r}$ ,  $D \in \mathbb{R}^{n \times r}$  and  $C \in \mathbb{R}^{p \times n}$  are constant system matrices.

*Remark 1:* As an effective method, NNs are widely applied in several fields of artificial intelligence and machine learning, such as computer vision, pattern recognition, and so on [27]. Different from these applications, this article studies the synchronization issue of two NN systems. Based on the dynamical properties (eg. oscillatory and chaos) of NNs, the studied synchronization issue of NNs can be used for image encryption and secure communication.

Combing (1) with (2), the synchronization error model is derived as

$$\begin{cases} \dot{x}(t) = -Ax(t) + u(t) + D\omega(t) + W_0\psi(x(t)) \\ \quad + W_1\psi(x(t-d)) + W_2 \int_{-d}^0 m(v)\psi(x(t+v))dv \\ z(t) = Cx(t) + E\omega(t) \end{cases} \quad (3)$$

where  $x(t) = \hat{y}(t) - y(t)$ ,  $z(t) = \hat{z}(t) - \bar{z}(t)$ ,  $\psi(x(t)) = \phi(\hat{y}(t)) - \phi(y(t))$  and  $\psi(x(t-d)) = \phi(\hat{y}(t-d)) - \phi(y(t-d))$ . The function  $\psi(x)$  and the distributed delay kernel  $m(v)$  satisfy the following assumptions, which are also used in [20] and [28], respectively.

*Assumption 1:* The function  $\psi(x)$  satisfies the following condition:

$$(\psi(x) - L_1x)^T(\psi(x) - L_2x) \leq 0 \quad (4)$$

where  $L_1$  and  $L_2$  are the two constant matrices satisfying  $L_2 - L_1 \geq 0$ .

*Assumption 2:* For the kernel  $m(v)$  of the distributed delay term  $\int_{-d}^0 m(v)\psi(x(t+v))dv$ , there exists a vector  $\mathbf{m}(v) = [m_0(v) \cdots m_i(v) \cdots m_\varrho(v)]^T$ ,  $m_0(v) \triangleq m(v)$ ,  $i = 0, 1, \dots, \varrho$  with  $\varrho \in \mathbb{N}$  and  $v \in [v_1, v_2]$  satisfying the following property:

$$\frac{d\mathbf{m}(v)}{dv} = \mathcal{M}\mathbf{m}(v) \quad (5)$$

where  $m_i(v)$  are linear independent,  $\mathcal{M} \in \mathbb{R}^{\varrho \times \varrho}$ , and  $\int_{v_1}^{v_2} \mathbf{m}(v)\mathbf{m}^T(v)dv > 0$ .

Assume that the states of master and slave systems are measured simultaneously and the measurements  $y(t_k)$  and  $\hat{y}(t_k)$  at time  $t_k$  ( $k \in \mathbb{N}$ ) are transmitted to the controller at the triggering

instants, which are determined by the following weighted IETS:

$$t_{k+1} = \min_t \{t \geq t_k + \eta | \epsilon^T(t) \Phi \epsilon(t) \geq \delta x(t_k)^T \Phi x(t_k)\} \quad (6)$$

where

$$\epsilon(t) = x^*(t) - x(t_k), x^*(t) \triangleq \int_{-h}^0 f(v)x(t+v)dv.$$

$t_k$  is the last triggering instant,  $t_{k+1}$  is the next triggering instant,  $\delta$  is a scalar belongs to  $[0, 1]$ ,  $\Phi > 0$  is the triggering matrix,  $\eta > 0$  is the waiting interval, and  $h > 0$  denotes the period of past system information. The weighting function,  $f(v)$ , similar to  $m(v)$ , is assumed to satisfy Assumption 2 with  $m(v)$  replaced by  $f(v)$ . In addition, without loss of generality, we assume  $\int_{-h}^0 f(v)dv = 1$ .

*Remark 2:* In some existing ETSs using instantaneous state  $x(t)$  to design the triggering rule, while the weighted mean of system state  $x^*(t)$  is utilized in the weighted IETS (6). The state of system may fluctuate frequently due to some external disturbances or noises. In this case, the existing ETSs based on  $x(t)$  may be sensitive to the fluctuations and trigger more control signals. However, taking the mean state can reduce the sensitivity of ETS to such fluctuations, which has the potential to decrease data transmission and save more communication and computation resources.

*Remark 3:* In the weighted IETS (6), a weighting function  $f(v)$  is introduced to weight the state of system at different instants. It has the effect of taking different weight of data, and is similar to the forgetting factor used in system identification [29] and Kalman filter [30], Laplacian kernel function used in quick pattern recognition [31], [32]. The weighting function  $f(v)$  is usually chosen as a decreasing function from current time  $t$  to previous time  $t - h$ . Namely, the importance of the error system state  $x(t + v)$  reduces as the decreasing of time from  $t$  to  $t - h$ .

*Remark 4:* If we choose the interval  $h = 0$ , (6) will reduce to the following switching ETS:

$$t_{k+1} = \min_t \{t \geq t_k + \eta | (x(t) - x(t_k))^T \Phi (x(t) - x(t_k)) \geq \delta x(t_k)^T \Phi x(t_k)\}. \quad (7)$$

The triggering threshold in (6) and (7) is  $\delta x(t_k)^T \Phi x(t_k)$ , which is different from  $\delta x(t)^T \Phi x(t)$  in the existing switching ETS [22], [24]. For the existing switching ETS [22], [24], the triggering threshold  $\delta x(t)^T \Phi x(t)$  needs to be calculated all the time when the triggering condition is executed. However, the triggering threshold  $\delta x(t_k)^T \Phi x(t_k)$  in (6) and (7) only needs to be computed one time at the triggering instant  $t_k$ , which can reduce the computation burden.

If the above weighted IETS is triggered at the instant  $t_k$ , the measurements  $y(t_k)$  and  $\hat{y}(t_k)$  are sent to the synchronizing controller, which is described as

$$u(t) = K(\hat{y}(t_k) - y(t_k)) = Kx(t_k), t \in [t_k, t_{k+1}) \quad (8)$$

where the controller gain  $K$  needs to be designed.

Then, the synchronization error system is given as

$$\begin{cases} \dot{x}(t) = -Ax(t) + W_0\psi(x(t)) + W_1\psi(x(t-d)) \\ \quad + W_2 \int_{-d}^0 m(v)\psi(x(t+v))dv \\ \quad + \chi(t)Kx(t-\tau(t)) + D\omega(t) \\ \quad + (1-\chi(t))K \left( \int_{-h}^0 f(v)x(t+v)dv - \epsilon(t) \right) \\ z(t) = Cx(t) + E\omega(t) \end{cases} \quad (9)$$

where

$$\chi(t) = \begin{cases} 1, & t \in [t_k, t_k + \eta) \\ 0, & t \in [t_k + \eta, t_{k+1}) \end{cases}$$

$$\tau(t) = t - t_k, t \in [t_k, t_k + \eta)$$

$$\epsilon(t) = \int_{-h}^0 f(v)x(t+v)dv - x(t_k), t \in [t_k + \eta, t_{k+1}).$$

This article aims to obtain a controller (8) such that

1) for  $\omega(t) = 0$ , the closed-loop system (9) is exponentially stable;

2) for any nonzero  $\omega(t)$  and zero initial condition, the control output  $z(t)$  meets  $\int_0^\infty z^T(t)z(t)dt < \gamma^2 \int_0^\infty \omega^T(t)\omega(t)dt$  with a given  $H_\infty$  index  $\gamma > 0$ .

Before ending this section, some technique lemmas are provided as follows.

*Lemma 1:* [28] For a positive symmetric matrix  $\mathcal{U} \in \mathbb{R}^{n \times n}$ , the defined  $\mathbf{m}(v)$  in Assumption 2, we have

$$\int_{v_1}^{v_2} x^T(v)\mathcal{U}x(v)dv \geq [*](\mathcal{R} \otimes \mathcal{U}) \int_{v_1}^{v_2} M(v)x(v)dv \quad (10)$$

with  $\mathcal{R}^{-1} = \int_{v_1}^{v_2} \mathbf{m}(v)\mathbf{m}^T(v)dv > 0$ ,  $M(v) = \mathbf{m}(v) \otimes I_n$ .

### III. MAIN RESULTS

To achieve the purpose of guaranteeing the exponential stability for the closed-loop system (9) with a required  $H_\infty$  index  $\gamma$ , we construct an LKF as

$$V(t) = \sum_{i=1}^5 V_i(t) \quad (11)$$

where

$$V_1(t) = \zeta^T(t)P_N\zeta^T(t), \zeta^T(t) = \begin{bmatrix} x(t) \\ \int_{-h}^0 F(v)x(t+v)dv \\ \int_{-d}^0 M(v)\psi(x(t+v))dv \end{bmatrix}$$

$$V_2(t) = \int_{t-h}^t e^{2\sigma(v-t)}x^T(v)[S_1 + (v-t+h)R_1]x(v)dv$$

$$V_3(t)$$

$$= \int_{t-d}^t e^{2\sigma(v-t)}\phi^T(x(v))[S_2 + (v-t+d)R_2]\phi(x(v))dv$$

$$V_4(t) = \int_{t-\eta}^t e^{2\sigma(v-t)}x^T(v)Q_1x(v)dv$$

$$V_5(t) = \int_{-\eta}^0 \int_{t+\theta}^t e^{2\sigma(v-t)}\dot{x}^T(v)Q_2\dot{x}(v)dv d\theta$$

$$F(v) \triangleq \mathbf{f}(v) \otimes I_n, f_1(v) = f(v)$$

$$\mathbf{f}(v) = [f_1(v), f_2(v), \dots, f_{\varrho_1}(v)]^T$$

$$M(v) \triangleq \mathbf{m}(v) \otimes I_n, m_1(v) = m(v)$$

$$\mathbf{m}(v) = [m_1(v), m_2(v), \dots, m_{\varrho_2}(v)]^T.$$

Based on  $F(v)$  and  $M(v)$  defined in (11), one obtains

$$\int_{-h}^0 f(v)x(t+v)dv = \int_{-h}^0 \mathcal{I}_1 F(v)x(t+v)dv \quad (12)$$

$$\int_{-d}^0 m(v)x(t+v)dv = \int_{-d}^0 \mathcal{I}_2 M(v)x(t+v)dv \quad (13)$$

with  $\mathcal{I}_1 = [I_n \ 0_{n,\varrho_1 n}]$  and  $\mathcal{I}_2 = [I_n \ 0_{n,\varrho_2 n}]$ .

Substituting (12) and (13) into (9), the closed-loop system is further expressed as

$$\begin{cases} \dot{x}(t) = -Ax(t) + W_0\psi(x(t)) + W_1\psi(x(t-d)) \\ \quad + W_2\mathcal{I}_2 \int_{-d}^0 M(v)\psi(x(t+v))dv \\ \quad + \alpha(t)Kx(t-\tau(t)) + D\omega(t) \\ \quad + (1-\alpha(t))K\mathcal{I}_1 \left( \int_{-h}^0 F(v)x(t+v)dv - \epsilon(t) \right) \\ z(t) = Cx(t) + E\omega(t). \end{cases} \quad (14)$$

First, we establish the exponential  $H_\infty$  stability criterion for the system (14) with the weighted IETS (6) in Theorem 1.

*Theorem 1:* For given parameters  $b_1, b_2, \delta, \eta, h, \rho, \sigma, \gamma$ , and controller gain  $K$ , under the weighted IETS (6), the system (14) is exponentially stable with the decay  $\sigma$  and required  $H_\infty$  index  $\gamma$ , if there exist symmetric matrices  $P_\varrho, S_1 > 0, R_1 > 0, S_2 > 0, R_2 > 0, Q_1 > 0, Q_2 > 0, \Phi > 0$ , and matrices  $X, N$  such that

$$\hat{P}_\varrho > 0 \quad (15)$$

$$\Xi + He(\mathcal{X}_1\mathcal{Y}_1) < 0 \quad (16)$$

$$\Theta + He(\mathcal{X}_2\mathcal{Y}_2) < 0 \quad (17)$$

where

$$\hat{P}_\varrho = P_\varrho + \text{diag}\{0, e^{-2\sigma h}(\mathcal{R}_1 \otimes S_1), e^{-2\sigma d}(\mathcal{R}_2 \otimes S_2)\}$$

$$\mathcal{R}_1^{-1} = \int_{-h}^0 \mathbf{f}(v)\mathbf{f}^T(v)dv, \mathcal{R}_2^{-1} = \int_{-d}^0 \mathbf{m}(v)\mathbf{m}^T(v)dv$$

$$\Xi = \begin{bmatrix} \Xi_1 & \Xi_2 \\ \Xi_2^T & -I \end{bmatrix}, \bar{L} = \begin{bmatrix} \bar{L}_1 & \bar{L}_2 \\ \bar{L}_2^T & I \end{bmatrix}$$

$$\bar{L}_1 = \frac{L_1^T L_2 + L_2^T L_1}{2}, \bar{L}_2 = \frac{L_1^T + L_2^T}{2}$$

$$\Xi_1 = He(H_1^T P_\varrho J_1 + 2\sigma H_1^T P_\varrho H_1)$$

$$- e^{-2\sigma s} \mathcal{E}_1^T \begin{bmatrix} Q_2 & N \\ N^T & Q_2 \end{bmatrix} \mathcal{E}_1 - \rho \mathcal{E}_2^T \bar{L} \mathcal{E}_2$$

$$+ \text{diag}\{\Xi_{11}, \Xi_{12}, 0_n, \Xi_{14}, \Xi_{15}, \Xi_{16}, \Xi_{17}, \Xi_{18}, \Xi_{19}, \Xi_{110}\}$$

$$\Xi_2^T = [0_{p,n} \ C \ 0_{p,5n} \ 0_{p,(\varrho_1+1)n} \ 0_{p,(\varrho_2+1)n} \ E]$$

$$\mathcal{E}_1 = \begin{bmatrix} 0_n & I_n & -I_n & 0_n & 0_{n,(\varrho_1+\varrho_2+5)n} & 0_{n,r} \\ 0_n & 0_n & I_n & -I_n & 0_{n,(\varrho_1+\varrho_2+5)n} & 0_{n,r} \end{bmatrix}$$

$$\mathcal{E}_2 = \begin{bmatrix} 0_n & I_n & 0_{n,3n} & 0_n & 0_{n,(\varrho_1+\varrho_2+3)n} & 0_{n,r} \\ 0_n & 0_n & 0_{n,3n} & I_n & 0_{n,(\varrho_1+\varrho_2+3)n} & 0_{n,r} \end{bmatrix}$$

$$\Xi_{11} = sQ_2, \Xi_{12} = Q_1 + S_1 + hR_1, \Xi_{14} = -e^{-2\sigma s}Q_1$$

$$\Xi_{15} = -e^{-2\sigma h}S_1, \Xi_{16} = S_2 + dR_2, \Xi_{17} = -e^{-2\sigma d}S_2$$

$$\Xi_{18} = -e^{-2\sigma h}(\mathcal{R}_1 \otimes R_1), \Xi_{19} = -e^{-2\sigma d}(\mathcal{R}_2 \otimes R_2)$$

$$\Xi_{110} = -\gamma^2 I, J_1 = [J_{11} \ J_{12} \ J_{13}], H_1 = [H_{11} \ H_{12}]$$

$$J_{11} = \begin{bmatrix} I_n & 0_n & 0_{n,2n} \\ 0_{(\varrho_1+1)n,n} & F(0) & 0_{(\varrho_1+1)n,2n} \\ 0_{(\varrho_2+1)n,n} & 0_{(\varrho_2+1)n,n} & 0_{(\varrho_2+1)n,2n} \end{bmatrix}$$

$$J_{12} = \begin{bmatrix} 0_n & 0_n & 0_n \\ -F(-h) & 0_{(\varrho_1+1)n,n} & 0_{(\varrho_1+1)n,n} \\ 0_{(\varrho_2+1)n,n} & M(0) & -M(-d) \end{bmatrix}$$

$$J_{13} = \begin{bmatrix} 0_n & 0_n & 0_{n,r} \\ -\hat{\mathcal{F}} & 0_{(\varrho_1+1)n,(\varrho_2+1)n} & 0_{(\varrho_1+1)n,r} \\ 0_{(\varrho_2+1)n,(\varrho_1+1)n} & -\hat{\mathcal{M}} & 0_{(\varrho_2+1)n,r} \end{bmatrix}$$

$$H_{11} = \begin{bmatrix} 0_n & I_n & 0_{n,5n} \\ 0_{(\varrho_1+1)n,n} & 0_{(\varrho_1+1)n,n} & 0_{(\varrho_1+1)n,5n} \\ 0_{(\varrho_2+1)n,n} & 0_{(\varrho_1+1)n,n} & 0_{(\varrho_2+1)n,5n} \end{bmatrix}$$

$$H_{12} = \begin{bmatrix} 0_{n,(\varrho_1+1)n} & 0_{n,(\varrho_2+1)n} & 0_{n,r} \\ I_{(\varrho_1+1)n} & 0_{(\varrho_1+1)n,(\varrho_2+1)n} & 0_{(\varrho_1+1)n,r} \\ 0_{(\varrho_2+1)n,(\varrho_1+1)n} & I_{(\varrho_2+1)n} & 0_{(\varrho_2+1)n,r} \end{bmatrix}$$

$$\hat{\mathcal{M}} = \mathcal{M} \otimes I_{(\varrho_1+1)n}, \hat{\mathcal{F}} = \mathcal{F} \otimes I_{(\varrho_2+1)n}$$

$$\mathcal{X}_1 = [b_1 X^T \ b_2 X^T \ 0_{n,5n} \ 0_{n,(\varrho_1+\varrho_2+2)n} \ 0_{n,r+p}]^T$$

$$\mathcal{Y}_1 = [-I \ -A \ K \ 0_{n,2n} \ W_0 \ W_1 \ 0_{n,(\varrho_1+1)n} \ W_2 \mathcal{I}_2 \ D \ 0_{n,p}]$$

$$\Theta = \begin{bmatrix} \Theta_1 & \Theta_2 \\ \Theta_2^T & -I \end{bmatrix}, \Theta_2 = \Xi_2$$

$$\Theta_1 = He(H_2^T P_\varrho J_2 + 2\sigma H_2^T P_\varrho H_2)$$

$$- e^{-2\sigma s} \mathcal{E}_3^T Q_2 \mathcal{E}_3 - \rho \mathcal{E}_4^T \bar{L} \mathcal{E}_4 + \delta \mathcal{E}_5^T \Phi \mathcal{E}_5$$

$$+ \text{diag}\{\Theta_{11}, \Theta_{12}, \Theta_{13}, \Theta_{14}, \Theta_{15}, \Theta_{16}, \Theta_{17}, \Theta_{18}, \Theta_{19}, \Theta_{110}\}$$

$$\mathcal{E}_3 = [0_n \ I_n \ -I_n \ 0_{n,3n} \ 0_{n,(\varrho_1+\varrho_2+2)n} \ 0_n \ 0_{n,r}]$$

$$\mathcal{E}_4 = \begin{bmatrix} 0_n & I_n & 0_{n,2n} & 0_n & 0_{n,(\varrho_1+\varrho_2+4)n} & 0_{n,r} \\ 0_n & 0_n & 0_{n,2n} & I_n & 0_{n,(\varrho_1+\varrho_2+4)n} & 0_{n,r} \end{bmatrix}$$

$$\mathcal{E}_5 = [0_{n,6n} \ \mathcal{I}_1 \ 0_{n,(\varrho_2+1)n} \ -I_n \ 0_{n,r}]$$

$$\Theta_{11} = sQ_2, \Theta_{12} = Q_1 + S_1 + hR_1, \Theta_{13} = -2e^{-2\sigma s}Q_1$$

$$\Theta_{14} = -e^{-2\sigma h}S_1, \Theta_{15} = S_1 + dR_1, \Theta_{16} = -e^{-2\sigma d}S_2$$

$$\Theta_{17} = -e^{-2\sigma h}(\mathcal{R}_1 \otimes R_1), \Theta_{18} = -e^{-2\sigma d}(\mathcal{R}_2 \otimes R_2)$$

$$\Theta_{19} = -\Phi, \Theta_{110} = -\gamma^2 I$$

$$\begin{aligned}
 J_2 &= \begin{bmatrix} J_{21} & J_{22} & J_{23} \end{bmatrix}, H_2 = \begin{bmatrix} H_{21} & H_{22} \end{bmatrix} \\
 J_{21} &= \begin{bmatrix} I_n & 0_n & 0_n & 0_n \\ 0_{(\varrho_1+1)n,n} & F(0) & 0_{(\varrho_1+1)n,n} & -F(-h) \\ 0_{(\varrho_2+1)n,n} & 0_{(\varrho_2+1)n,n} & 0_{(\varrho_1+2)n,n} & 0_{(\varrho_2+1)n,n} \end{bmatrix} \\
 J_{22} &= \begin{bmatrix} 0_n & 0_n & 0_n \\ 0_{(\varrho_1+1)n,n} & 0_{(\varrho_1+1)n,n} & -\widehat{\mathcal{F}} \\ M(0) & -M(-d) & 0_{(\varrho_2+1)n,(\varrho_1+1)n} \end{bmatrix} \\
 J_{23} &= \begin{bmatrix} 0_n & 0_n & 0_{n,r} \\ 0_{(\varrho_1+1)n,(\varrho_2+1)n} & 0_{(\varrho_1+1)n,n} & 0_{(\varrho_1+1)n,r} \\ -\widehat{\mathcal{M}} & 0_{(\varrho_2+1)n,n} & 0_{(\varrho_2+1)n,r} \end{bmatrix} \\
 H_{21} &= \begin{bmatrix} 0_n & I_n & 0_{n,4n} \\ 0_{(\varrho_1+1)n,n} & 0_{(\varrho_1+1)n,n} & 0_{(\varrho_1+1)n,4n} \\ 0_{(\varrho_2+1)n,n} & 0_{(\varrho_1+1)n,n} & 0_{(\varrho_2+1)n,4n} \end{bmatrix} \\
 H_{22} &= \begin{bmatrix} 0_{n,(\varrho_1+1)n} & 0_{n,(\varrho_2+1)n} & 0_{n,n+r} \\ I_{(\varrho_1+1)n} & 0_{(\varrho_1+1)n,(\varrho_2+1)n} & 0_{(\varrho_1+1)n,n+r} \\ 0_{(\varrho_2+1)n,(\varrho_1+1)n} & I_{(\varrho_2+1)n} & 0_{(\varrho_2+1)n,n+r} \end{bmatrix} \\
 \mathcal{X}_2 &= \begin{bmatrix} b_1 X^T & b_2 X^T & 0_{n,4n} & 0_{n,(\varrho_1+\varrho_2+3)n} & 0_{n,r+p} \end{bmatrix}^T \\
 \mathcal{Y}_2 &= \begin{bmatrix} -I_n & -A & 0_{n,2n} & W_0 & W_1 & K\mathcal{I}_1 \\ W_2\mathcal{I}_2 & -K & D & 0_{n,p} \end{bmatrix}.
 \end{aligned}$$

*Proof:* For the chosen LKF (11), by applying Lemma 1, it yields that

$$\begin{aligned}
 &\int_{-h}^0 e^{2\sigma v} x^T(t+v) S_1 x(t+v) dv \\
 &\geq e^{-2\sigma h} [*](\mathcal{R}_1 \otimes S_1) \int_{-h}^0 F(v) x(t+v) dv \quad (18)
 \end{aligned}$$

$$\begin{aligned}
 &\int_{-d}^0 e^{2\sigma v} \psi^T(x(t+v)) S_2 \psi(x(t+v)) dv \\
 &\geq e^{-2\sigma d} [*](\mathcal{R}_2 \otimes S_2) \int_{-d}^0 M(v) \psi(x(t+v)) dv. \quad (19)
 \end{aligned}$$

Therefore, from (11), (18), and (19), one has

$$\begin{aligned}
 V(t) &\geq \zeta^T(t) \hat{P}_\varrho \zeta(t) \\
 &+ \int_{-h}^0 e^{2\sigma v} x^T(t+v) (v+h) R_1 x(t+v) dv \\
 &+ \int_{-d}^0 e^{2\sigma v} \psi^T(x(t+v)) (v+d) R_2 \psi(x(t+v)) dv \\
 &+ \int_{-\eta}^0 e^{2\sigma v} x^T(t+v) Q_1 x(t+v) dv \\
 &+ \int_{-\eta}^0 \int_{t+\theta}^t e^{2\sigma(v-t)} \dot{x}^T(v) Q_2 \dot{x}(v) dv d\theta. \quad (20)
 \end{aligned}$$

From  $S_1 > 0, R_1 > 0, S_2 > 0, R_2 > 0, Q_1 > 0, Q_2 > 0$  and  $\hat{P}_\varrho > 0, V(t)$  is ensured to be positive.

Based on Assumption 2, one obtains

$$\begin{aligned}
 &\frac{d}{dt} \int_{-h}^0 F(v) x(t+v) dv = F(0) x(t) \\
 &- F(-h) x(t-h) - \widehat{\mathcal{F}} \int_{-h}^0 F(v) x(t+v) dv \quad (21)
 \end{aligned}$$

$$\begin{aligned}
 &\frac{d}{dt} \int_{-d}^0 M(v) \psi(x(t+v)) dv = M(0) \psi(x(t)) \\
 &- M(-d) \psi(x(t-d)) - \widehat{\mathcal{M}} \int_{-d}^0 M(v) \psi(x(t+v)) dv \quad (22)
 \end{aligned}$$

where  $\widehat{\mathcal{F}} = \mathcal{F} \otimes I_{(\varrho_2+1)n}, \widehat{\mathcal{M}} = \mathcal{M} \otimes I_{(\varrho_1+1)n}$ .

Then, in order to meet  $H_\infty$  performance, it requires the derivative of  $V(t)$  to satisfy

$$\begin{aligned}
 &\dot{V}(t) + 2\sigma V(t) + z^T(t) z(t) - \gamma^2 \omega^T(t) \omega(t) \\
 &\leq 2\zeta^T(t) P_N \dot{\zeta}(t) + 2\sigma \zeta^T(t) P_N \zeta(t) \\
 &+ x^T(t) (S_1 + hR_1) x(t) - e^{-2\sigma h} x^T(t-h) S_1 x(t-h) \\
 &+ \psi^T(x(t)) (S_2 + dR_2) \psi(x(t)) \\
 &- e^{-2\sigma d} \psi^T(x(t-d)) S_2 \psi(x(t-d)) \\
 &+ x^T(t) Q_1 x(t) - e^{-2\sigma \eta} x^T(t-\eta) Q_1 x(t-\eta) \\
 &+ \eta \dot{x}^T(t) Q_2 \dot{x}(t) + z^T(t) z(t) - \gamma^2 \omega^T(t) \omega(t) \\
 &- e^{-2\sigma h} \int_{-h}^0 x^T(t+v) R_1 x(t+v) dv \\
 &- e^{-2\sigma d} \int_{-d}^0 \psi^T(x(t+v)) R_2 \psi(x(t+v)) dv \\
 &- e^{-2\sigma \eta} \int_{t-\eta}^t \dot{x}^T(v) Q_2 \dot{x}(v) dv < 0. \quad (23)
 \end{aligned}$$

Using Lemma 1 to relax the integral terms in (23), one has

$$\begin{aligned}
 &- e^{-2\sigma h} \int_{-h}^0 x^T(t+v) R_1 x(t+v) dv \\
 &\leq -e^{-2\sigma h} \int_{-h}^0 [*](\mathcal{R}_1 \otimes R_1) F(v) x(t+v) dv \quad (24) \\
 &- e^{-2\sigma d} \int_{-d}^0 \psi^T(x(t+v)) R_2 \psi(x(t+v)) dv \\
 &\leq -e^{-2\sigma d} \int_{-d}^0 [*](\mathcal{R}_2 \otimes R_2) M(v) \psi(x(t+v)) dv. \quad (25)
 \end{aligned}$$

Next, two switching system modes under the waiting period and execution of event triggering are considered, respectively.

Case A: The system (14) with  $\chi(t) = 1$ ,  $t \in [t_k, t_k + \eta)$  is described as

$$\begin{cases} \dot{x}(t) = -Ax(t) + W_0\psi(x(t)) + W_1\psi(x(t-d)) \\ \quad + W_2\mathcal{I}_2 \int_{-d}^0 M(v)\psi(x(t+v))dv \\ \quad + Kx(t-\tau(t)) + D\omega(t) \\ z(t) = Cx(t) + E\omega(t). \end{cases} \quad (26)$$

From (26), one obtains  $\zeta(t) = H_1\xi_1(t)$  and  $\dot{\zeta}(t) = J_1\xi_1(t)$  with  $\xi_1^T(t) = [\dot{x}^T(t)x^T(t)x^T(t-\tau(t))x^T(t-\eta)x^T(t-h)\psi^T(x(t))\psi^T(x(t-d)) \int_{-h}^0 (F(v)x(t+v))^T dv \int_{-d}^0 (M(v)x(t+v))^T dv \omega^T(t)]$ .

In terms of the well-known reciprocally convex lemma [34], one can get

$$\begin{aligned} & -e^{-2\sigma\eta} \int_{t-\eta}^t \dot{x}^T(v)Q_2\dot{x}(v)dv \\ & \leq -e^{-2\sigma\eta}\xi_1^T(t)\mathcal{E}_1^T \begin{bmatrix} Q_2 & N \\ N^T & Q_2 \end{bmatrix} \mathcal{E}_1\xi_1(t). \end{aligned} \quad (27)$$

Resorting to Assumption 1, it gives

$$\begin{bmatrix} x^T(t) & \psi^T(x(t)) \end{bmatrix} \begin{bmatrix} \bar{L}_1 & \bar{L}_2 \\ \bar{L}_2^T & I \end{bmatrix} \begin{bmatrix} x(t) \\ \psi(x(t)) \end{bmatrix} \leq 0 \quad (28)$$

for any  $\rho > 0$ , which leads to

$$-\rho\xi_1^T(t)\mathcal{E}_2^T\bar{L}\mathcal{E}_2\xi_1(t) \geq 0. \quad (29)$$

Combining (24), (25), (27), and (29) gives

$$\hat{\xi}_1^T(t)\Xi\hat{\xi}_1(t) < 0 \quad (30)$$

which further makes (23) hold with  $\hat{\xi}_1^T(t) = [\xi_1^T(t) z^T(t)]$ .

Revisiting the description of system (26) and applying the well-known Finsler lemma in [33], it yields

$$\hat{\xi}_1^T(t)(\Xi + He(\mathcal{X}_1\mathcal{Y}_1))\hat{\xi}_1(t) < 0 \quad (31)$$

which is equivalent to (16).

Case B: The system (14) with  $\chi(t) = 0$ ,  $t \in [t_k + \eta, t_{k+1})$  is given as

$$\begin{cases} \dot{x}(t) = -Ax(t) + W_0\psi(x(t)) + W_1\psi(x(t-d)) \\ \quad + W_2\mathcal{I}_2 \int_{-d}^0 M(v)\psi(x(t+v))dv + D\omega(t) \\ \quad + K\mathcal{I}_1 \left( \int_{-h}^0 F(v)x(t+v)dv - \epsilon(t) \right) \\ z(t) = Cx(t) + E\omega(t). \end{cases} \quad (32)$$

From (32), we have

$$\zeta(t) = H_2\xi_2(t), \dot{\zeta}(t) = J_2\xi_2(t) \quad (33)$$

where  $\xi_2^T(t) = [\dot{x}^T(t)x^T(t)x^T(t-\eta)x^T(t-h)\psi^T(x(t))\psi^T(x(t-d)) \int_{-h}^0 (F(v)x(t+v))^T dv \int_{-d}^0 (M(v)x(t+v))^T dv \epsilon^T(t)\omega^T(t)]$ .

Resorting to Assumption 1 and  $\xi_2(t)$  defined in (33), (29) in Case A is rewritten as

$$-\rho\xi_2^T(t)\mathcal{E}_4^T\bar{L}\mathcal{E}_4\xi_2(t) \geq 0. \quad (34)$$

In terms of Jensen inequality [36], one can derive

$$\begin{aligned} & -e^{-2\sigma\eta} \int_{-h}^0 \dot{x}^T(t+v)Q_2\dot{x}(t+v)dv \\ & \leq -e^{-2\sigma\eta}\xi_2^T(t)\mathcal{E}_3^T Q_2\mathcal{E}_3\xi_2(t). \end{aligned} \quad (35)$$

For Case B with the time interval  $[t_k + \eta, t_{k+1})$ , the weighted IETS (6) is not triggered, which means

$$\epsilon^T(t)\Phi\epsilon(t) < \delta x^T(t_k)\Phi x(t_k). \quad (36)$$

Since  $\epsilon(t) = x^*(t) - x(t_k)$  in (6) with  $x^*(t) \triangleq \int_{-h}^0 f(v)x(t+v)dv$ , one can express  $x(t_k) = x^*(t) - \epsilon(t)$ . With this expression, we have

$$\begin{aligned} \epsilon^T(t)\Phi\epsilon(t) & < \delta[*]\Phi \left( \int_{-h}^0 f(v)x(t+v)dv - \epsilon(t) \right) \\ & = \delta[*]\Phi \left( \mathcal{I}_1 \int_{-h}^0 F(v)x(t+v)dv - \epsilon(t) \right) \end{aligned} \quad (37)$$

where  $\mathcal{I}_1 = [I_n \ 0_{n,\varrho_1n}]$  is defined in (12).

Utilizing the notations  $\mathcal{E}_5 = [0_{n,6n} \ \mathcal{I}_1 \ 0_{n,(\varrho_2+1)n} \ -I_n \ 0_{n,r}]$  given in Theorem 1 and  $\xi_2(t)$  in (33), one can obtain  $\mathcal{I}_1 \int_{-h}^0 F(v)x(t+v)dv - \epsilon(t) = \mathcal{E}_5\xi_2(t)$ . Then, (37) is rewritten as

$$\epsilon^T(t)\Phi\epsilon(t) < \delta\xi_2^T(t)\mathcal{E}_5^T\Phi\mathcal{E}_5\xi_2(t). \quad (38)$$

Adding and subtracting  $\epsilon^T(t)\Phi\epsilon(t)$  to and from (23), and using (38), it yields

$$\begin{aligned} & \dot{V}(t) + 2\sigma V(t) + z^T(t)z(t) - \gamma^2\omega^T(t)\omega(t) \\ & \quad + \epsilon^T(t)\Phi\epsilon(t) - \epsilon^T(t)\Phi\epsilon(t) \\ & \leq 2\zeta^T(t)P_N\dot{\zeta}(t) + 2\sigma\zeta^T(t)P_N\zeta(t) \\ & \quad + x^T(t)(S_1 + hR_1)x(t) - e^{-2\sigma h}x^T(t-h)S_1x(t-h) \\ & \quad + \psi^T(x(t))(S_2 + dR_2)\psi(x(t)) \\ & \quad - e^{-2\sigma d}\psi^T(x(t-d))S_2\psi(x(t-d)) \\ & \quad + x^T(t)Q_1x(t) - e^{-2\sigma\eta}x^T(t-\eta)Q_1x(t-\eta) \\ & \quad + \eta\dot{x}^T(t)Q_2\dot{x}(t) + z^T(t)z(t) - \gamma^2\omega^T(t)\omega(t) \\ & \quad - e^{-2\sigma h} \int_{-h}^0 x^T(t+v)R_1x(t+v)dv \\ & \quad - e^{-2\sigma d} \int_{-d}^0 \psi^T(x(t+v))R_2\psi(x(t+v))dv \\ & \quad - e^{-2\sigma\eta} \int_{t-\eta}^t \dot{x}^T(v)Q_2\dot{x}(v)dv \\ & \quad + \delta\xi_2^T(t)\mathcal{E}_5^T\Phi\mathcal{E}_5\xi_2(t) - \epsilon^T(t)\Phi\epsilon(t) < 0. \end{aligned} \quad (39)$$

Based on (24), (25), (32)–(39), and following the similar way in Case A, one can get

$$\hat{\xi}_2^T(t)(\Theta + He(\mathcal{X}_2\mathcal{Y}_2))\hat{\xi}_2(t) < 0 \quad (40)$$

with  $\hat{\xi}_2^T(t) = [\xi_2^T(t) z^T(t)]$ , which is guaranteed by (17). ■

*Remark 5:* With the help of condition (15), the Lyapunov variable  $P_\varrho$  is not required to be positive to ensure the positivity of the chosen LKF (11). Then less conservative stability conditions can be derived than some existing results needing all Lyapunov variables to be positive.

Second, sufficient conditions for designing an event-triggered controller are derived in Theorem 2.

*Theorem 2:* For given scalars  $b_1, b_2, \delta, \eta, h, \rho, \sigma, \gamma$ , under the weighted IETS (6), the system (14) is exponentially stable with the decay  $\sigma$  and required  $H_\infty$  index  $\gamma$ , if there exist symmetric matrices  $P_\varrho, S_1 > 0, R_1 > 0, S_2 > 0, R_2 > 0, Q_1 > 0, Q_2 > 0, \Phi > 0$  and matrices  $X, N, Y$  such that (15) and

$$\Xi + He(\hat{\mathcal{X}}_1 \hat{\mathcal{Y}}_1) < 0 \quad (41)$$

$$\Theta + He(\hat{\mathcal{X}}_2 \hat{\mathcal{Y}}_2) < 0 \quad (42)$$

where

$$\hat{\mathcal{X}}_1 = [b_1 I_n \quad b_2 I_n \quad 0_{n,5n} \quad 0_{n,(\varrho_1+\varrho_2+2)n} \quad 0_{n,r+p}]^T$$

$$\hat{\mathcal{Y}}_1 = [-X \quad -XA \quad Y \quad 0_{n,2n} \quad XW_0 \quad XW_1 \quad 0_{n,(N_1+1)n} \quad XW_2 \mathcal{I}_2 \quad XD \quad 0_{n,p}]$$

$$\hat{\mathcal{X}}_2 = [b_1 I \quad b_2 I \quad 0_{n,4n} \quad 0_{n,(\varrho_1+\varrho_2+2)n} \quad 0_n \quad 0_{n,r+p}]^T$$

$$\hat{\mathcal{Y}}_2 = [-X \quad -XA \quad 0_{n,2n} \quad XW_0 \quad XW_1 \quad Y \mathcal{I}_1 \quad XW_2 \mathcal{I}_2 \quad -Y \quad XD \quad 0_{n,p}].$$

Then, one can obtain the controller gain from  $K = X^{-1}Y$ .

*Proof:* By defining  $Y = XK$  as a novel variable and substituting it to (16) and (17), it leads to (41) and (42), respectively. This ends the proof.  $\blacksquare$

#### IV. NUMERICAL EXAMPLE

*Example 1:* Consider the same parameters with [35] of systems (1) and (2) with the following parameters:

$$A = \begin{bmatrix} 1 & 0 \\ 0 & 1 \end{bmatrix}, W_0 = \begin{bmatrix} 1.8 & -0.15 \\ -5.2 & 3.5 \end{bmatrix}$$

$$W_1 = \begin{bmatrix} -1.7 & -0.12 \\ -0.26 & -2.5 \end{bmatrix}, W_2 = \begin{bmatrix} 0.6 & 0.9 \\ -2 & -0.7 \end{bmatrix}$$

$$C = \begin{bmatrix} 1 & 0 \\ 0 & 1 \end{bmatrix}, D = \begin{bmatrix} 0.2 \\ 0.5 \end{bmatrix}, E = \begin{bmatrix} 0.2 \\ 1 \end{bmatrix}$$

and  $\psi(x_i) = \tanh(\hat{y}_i) - \tanh(y_i)$  satisfying Assumption 1 with  $L_1 = 0_2, L_2 = \begin{bmatrix} 1 & 0 \\ 0 & 1 \end{bmatrix}$ .

The distributed delay kernel is selected as  $m(v) = -50ve^{10v}, v \in [-d, 0]$  with  $\dot{m}(v) = 10(-50ve^{10v}) + (-50e^{10v})$ . According to Assumption 2, it is natural to add another term  $-50e^{10v}$  in  $\mathbf{m}(v)$  and give

$$\mathbf{m}(v) = \begin{bmatrix} -50ve^{10v} \\ -50e^{10v} \end{bmatrix}, \mathcal{M} = \begin{bmatrix} 10 & 1 \\ 0 & 10 \end{bmatrix}$$

$$M(v) = \mathbf{m}(v) \otimes I_2, \mathcal{I}_2 = [I_2 \quad 0_{n,\varrho_2 n}]$$

$$\widehat{\mathcal{M}} = \mathcal{M} \otimes I_2, \mathcal{R}_2 = \left( \int_{-d}^0 \mathbf{m}(v) \mathbf{m}^T(v) dv \right)^{-1}.$$

Two different weighting functions  $f(v), v \in [-h, 0]$  in the weighted IETS (6) with  $\int_{-h}^0 f(v) dv = 1$  are considered as

$$\text{Case 1: } f(v) = \frac{\pi}{2h} \cos\left(\frac{\pi}{2h}v\right), \mathcal{I}_1 = [I_n \quad 0_{n,\varrho_1 n}]$$

$$\mathbf{f}(v) = \begin{bmatrix} \frac{\pi}{2h} \cos\left(\frac{\pi}{2h}v\right) \\ \frac{\pi}{2h} \sin\left(\frac{\pi}{2h}v\right) \\ 1 \end{bmatrix}, \mathcal{F} = \begin{bmatrix} 0 & -\frac{\pi}{2h} & 0 \\ \frac{\pi}{2h} & 0 & 0 \\ 0 & 0 & 0 \end{bmatrix}$$

$$\text{Case 2: } f(v) = 2v/h^2 + 2/h, \mathcal{I}_1 = [I_n \quad 0_{n,\varrho_1 n}]$$

$$\mathbf{f}(v) = \begin{bmatrix} 2v/h^2 + 2/h \\ v^2/h^2 \\ 1/h \end{bmatrix}, \mathcal{F} = \begin{bmatrix} 0 & 0 & 2/h \\ 1 & 0 & -2 \\ 0 & 0 & 0 \end{bmatrix}.$$

Based on the same way for  $m(v)$ , it is easy to obtain

$$F(v) = \mathbf{f}(v) \otimes I_n, \widehat{\mathcal{F}} = \mathcal{F} \otimes I_n$$

$$\mathcal{R}_1 = \left( \int_{-h}^0 \mathbf{f}(v) \mathbf{f}^T(v) dv \right)^{-1}.$$

We choose  $d = 1, h = 0.03, \eta = 0.0075, b_1 = 1, b_2 = 10, \delta = 0.1, \sigma = 0.1$ , and  $\rho = 20$ . By solving Theorem 2 for Cases 1 and 2 under the same  $H_\infty$  index  $\gamma = 1$ , the controller gain  $K$  and triggering matrix  $\Phi$  are given as

$$K = \begin{bmatrix} -4.5974 & 0.4102 \\ -1.6917 & -5.6769 \end{bmatrix}, \Phi = \begin{bmatrix} 248.4862 & 34.9302 \\ 34.9302 & 33.3722 \end{bmatrix}$$

$$K = \begin{bmatrix} -4.7832 & 0.3287 \\ -1.9497 & -5.4826 \end{bmatrix}, \Phi = \begin{bmatrix} 270.7576 & 41.4568 \\ 41.4568 & 31.8353 \end{bmatrix}.$$

In simulation, we set initial conditions of the master system  $y(0) = [-0.5 \quad 0.2]^T$  and the slave system  $\hat{y}(0) = [0 \quad 0]^T$  and simulation step  $0.0025s$ . The exogenous disturbance is considered as  $\omega(t) = a(t)$  for  $0 < t < 3s$  ( $\omega(t) = 0$  for  $t \geq 3s$ ), where  $a(t)$  is a uniformly distributed random variable satisfying  $|a(t)| \leq 1$ . The unstable state trajectories of the master and slave systems and the error system (3) without synchronization control are drawn in Fig. 1. Under the weighted IETS and synchronization controller, the curves and release instants are shown in Fig. 2 for Case 1 and Fig. 3 for Case 2, respectively. It is seen from Fig. 1 that the master and slave systems cannot be synchronized without control signals. According to Figs. 2 and 3, however, the master system and the slave system are well synchronized via the controller (8) and the weighted IETS (6) when external disturbance occurs.

Next, when the weighting function  $f(v)$  is chosen as a constant  $1/h$ , the weighted IETS can be viewed as a conventional IETS with  $f(v) = \frac{1}{h}, \mathcal{I}_1 = [I_n \quad 0_{n \times \varrho_1 n}]$

$$\mathbf{f}(v) = \begin{bmatrix} 1/h \\ v/h \\ v^2/h \end{bmatrix}, \mathcal{F} = \begin{bmatrix} 0 & 0 & 0 \\ 1 & 0 & 0 \\ 0 & 2/h & 0 \end{bmatrix}.$$

To show the advantage of the introduced weighting function, the compared results between the weighted IETS with two

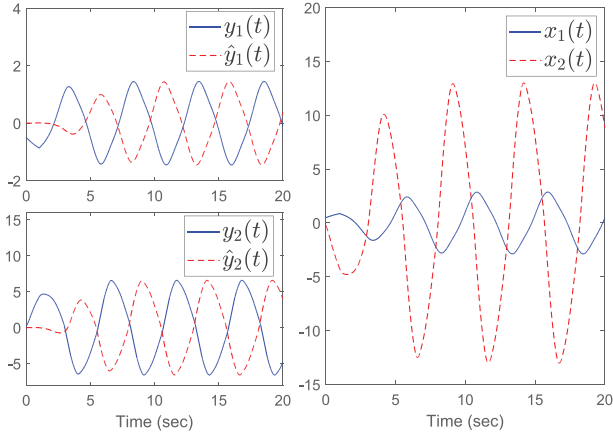


Fig. 1. Curves of  $y(t)$ ,  $\hat{y}(t)$ , and  $x(t)$  without control.

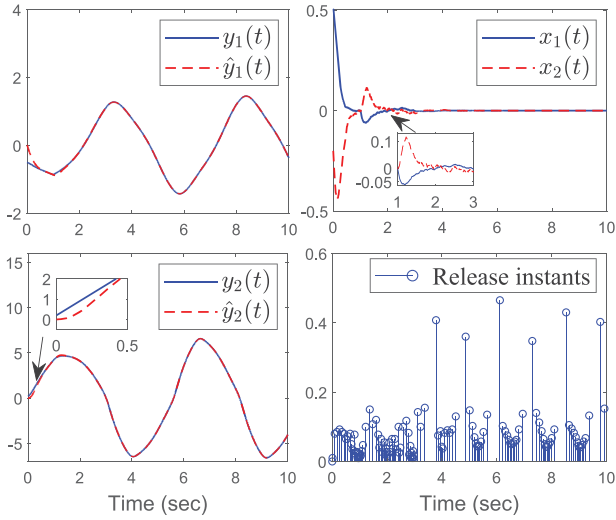


Fig. 2. Case 1: the curves of  $y(t)$ ,  $\hat{y}(t)$  and  $x(t)$  and the release instants with the weighted IETS (6) and controller (8).

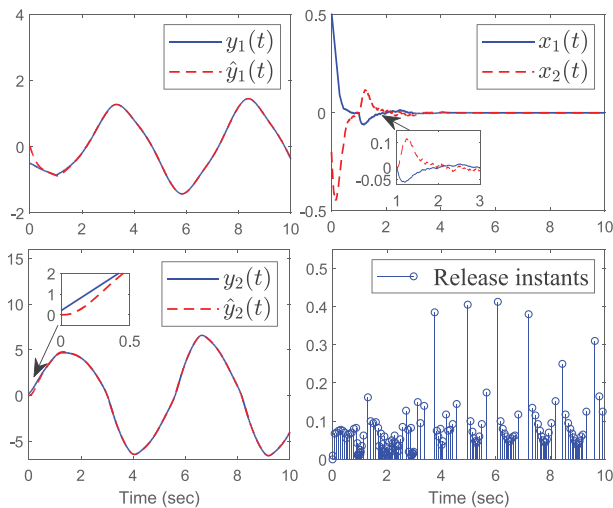


Fig. 3. Case 2: the curves of  $y(t)$ ,  $\hat{y}(t)$  and  $x(t)$  and the release instants with the weighted IETS (6) and controller (8).

TABLE I  
TOTAL EVENTS ( $\mathcal{N}$ ) UNDER THE SAME  $H_\infty$  INDEX  $\gamma = 1$

$\mathcal{N}$	Weighted IETS: Case 1	Weighted IETS: Case 2	Conventional IETS
$h = 0.02$	145	154	161
$h = 0.03$	129	135	149
$h = 0.05$	121	124	132

TABLE II  
 $H_\infty$  INDEX  $\gamma$  WITH THE SAME  $h = 0.05$

	Weighted IETS: Case 1	Weighted IETS: Case 2	Conventional IETS
$\gamma$	0.4556	0.4488	0.4658

different weighting functions and the conventional IETS are derived as below. Under the same  $H_\infty$  index  $\gamma = 1$  and the scalars chosen above, the numbers of total events generated by the weighted and conventional IETSs are shown in Table I. From Table I, under the same  $H_\infty$  performance, both Cases 1 and 2 of the weighted IETS generate fewer triggering events than the conventional IETS. For example, the number of total events generated by Case 1 is reduced by 9.94% ( $h = 0.02$ ), 13.42% ( $h = 0.03$ ) and 9.09% ( $h = 0.05$ ) compared to the one generated by the conventional IETS, respectively. Meanwhile, one can note that different  $h$  may lead to different triggering times, and the theoretic approach to select the optimum  $h$  needs further investigation in the future.

Moreover, to illustrate the impact of the weighting function on  $H_\infty$  performance, the index  $\gamma$  obtained by different IETSs is given in Table II. Based on Table II, it is seen that with the help of using weighting function, the values of  $\gamma$  obtained via Cases 1 and 2 of our weighted IETS are less than the  $H_\infty$  index derived by the conventional IETS. Consequently, these results illustrate the superiority of the weighted IETS.

## V. APPLICATION TO IMAGE ENCRYPTION

In this section, the developed event-triggered synchronization result of delayed NNs (3) derived from Theorem 2 is applied to image encryption issue. Before the image encryption, we choose the same parameters used for obtaining Fig. 2 and repeat the simulation process over time interval  $[0, 800s)$ . An iterative encryption algorithm executed on a color picture  $Pic$  of size  $m \times n \times 3$  is given as:

*Step 1:* Converting the color image  $Pic(i, j, l)$ ,  $i = 1, 2, \dots, m$ ,  $j = 1, 2, \dots, n$ ,  $l = 1, 2, 3$  into a matrix  $O(\alpha, \beta)$ , which is represented as

$$\begin{cases} Pic(\alpha, \beta, 1), \alpha = 1, \dots, m, \beta = 1, \dots, n \\ Pic(\alpha - m, \beta, 2), \alpha = m + 1, \dots, 2m, \beta = 1, \dots, n \\ Pic(\alpha - 2m, \beta, 3), \alpha = 2m + 1, \dots, 3m, \beta = 1, \dots, n. \end{cases} \quad (43)$$

*Step 2:* After system (9) is synchronized by the weighted IETS and synchronization controller at time instant  $k_1$ , three encryption keys based on the master system state variables  $y(t)$  are

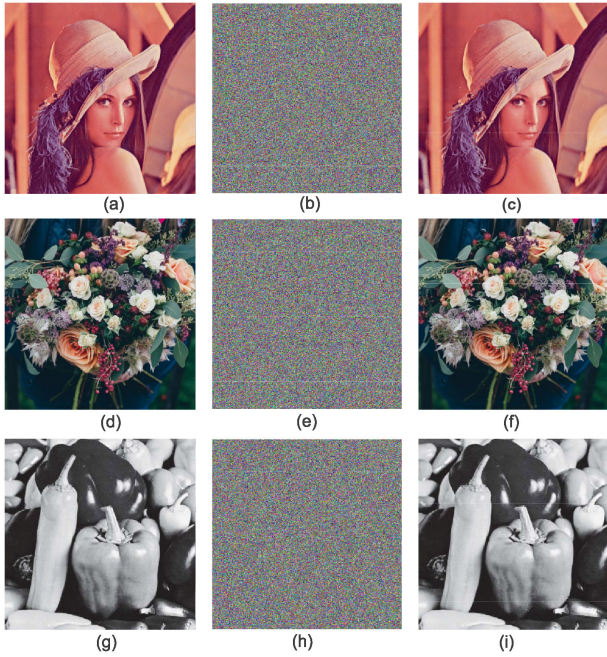


Fig. 4. Original, encrypted, and decrypted images of Lena, Flower, and Pepper under the encryption algorithm with  $\aleph = 2$ .

derived based on the master system state as

$$K_1(\alpha) = \text{mod}((10^5 \times |y_1(k_\alpha) + y_2(k_\alpha)| - \text{floor}(|y_1(k_\alpha) + y_2(k_\alpha)|), 3m) + 1) \quad (44)$$

$$K_2(\beta) = \text{mod}((10^5 \times |y_1(k_\beta) \times y_2(k_\beta)| - \text{floor}(|y_1(k_\beta) \times y_2(k_\beta)|), n) + 1) \quad (45)$$

$$K_3(q) = \text{mod}(10^5 \times |y_1(k_q) \times y_2(k_q)| - \text{floor}(|y_1(k_q) \times y_2(k_q)|), 256) \quad (46)$$

where  $k_\alpha \in \{k_1, k_2, \dots, k_{3m}\}$ ,  $k_\beta \in \{k_1, k_2, \dots, k_n\}$ ,  $k_q \in \{k_1, k_2, \dots, k_{256}\}$ .

Step 3: Substitute the  $\alpha$ th row and  $\beta$ th column by the  $K_1(\alpha)$ th row and the  $K_2(\beta)$ th column to  $O(\alpha, \beta)$ , and transform the matrix  $O(K_1(\alpha), K_2(\beta))$  into a row vector  $\mathcal{V}(i) \in \mathbb{R}^{1 \times 3mn}$ . With the help of the above encrypted keys, a novel vector  $\mathcal{V}'$  is generated as

$$\mathcal{V}'(i) = \mathcal{V}(i) \oplus (\mathcal{V}(i) + K_3(i)) \oplus \mathcal{V}'(i - 1) \quad (47)$$

for  $i = 1, \dots, 3mn$ , where  $\oplus$  means the logical operation. Then, rearranging the vector  $\mathcal{V}'$  into a picture of size  $m \times n \times 3$ .

Step 4: Repeat Steps 1–3 for  $\aleph$  times to derive the encrypted picture  $Pic$ .

Since the decryption process based on the state of slave system  $\hat{y}(t)$  is the reverse of the encryption, it is omitted here.

To demonstrate the effectiveness of our encryption algorithm, three different color images are used for evaluation. They are Lena, Flower, and Pepper, as shown in Fig. 4. The histograms of the red, green, and blue of the original Lena and the encrypted Lena are drawn in Fig. 5 with  $\aleph = 2$ . It is seen from Fig. 4 that the encrypted images can be decrypted well after the system

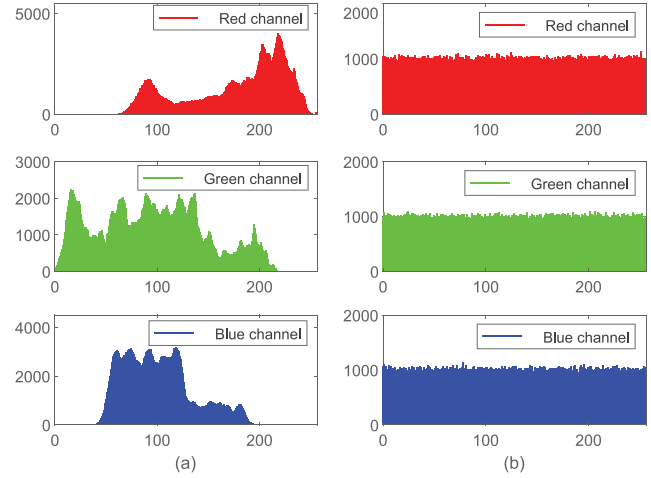


Fig. 5. Histograms of red, green, and blue components of (a) original Lena (b) and encrypted Lena.

TABLE III  
NPCR AND UACI OF THE ENCRYPTION ALGORITHMS

	Our algorithm with $\aleph = 1$	Our algorithm with $\aleph = 2$	Algorithm in [5]	Algorithm in [6]
NPCR	98.59%	99.62%	53.67%	54.81%
UACI	34.12%	33.45%	3.36%	0.43%

reached synchronization via the proposed encryption algorithm. Moreover, Fig. 5 shows that the histograms of the encrypted image are almost subject to uniform distribution. This indicates that the encryption algorithm makes the tonal distribution of the original image more stochastic, which improves the security of the encryption algorithm.

Next, to show the better security of the proposed encryption algorithm than some existing algorithms, the effect of the differential attack on encryption is analyzed. Attackers make a small change to the original image and discover the relationship between the original and encrypted images. Two indices, the number of pixel change rate (NPCR) and unified average changing intensity (UACI), are commonly utilized to evaluate the impact of one-pixel change on the encrypted image [37]. The ideal values of NPCR and UACI are 99.61% and 33.33%, respectively [37]. We change one pixel value  $Pic(125, 125, 2)$  into  $Pic(125, 125, 2) + 1$  of the original Lena. Then encrypt the original images with/without the change and compute NPCR and UACI of the encrypted images. The compared results of picture Lena are derived in Table III. This table illustrates that NPCR = 99.62% and UACI = 33.45% of our encryption algorithm with the iteration  $\aleph = 2$  are very close to their ideal values, which indicates the stronger ability against the differential attack of the proposed encryption algorithm than the algorithms in [5] and [6]. With the increase of iteration  $\aleph$ , the ideal quality of the proposed encryption algorithm can be reached gradually.

In addition, to ensure the synchronization of NNs that used for image encryption algorithm, an event-triggered communication strategy is adopted in this article, which is effective to reduce data transmission. However, a continuous communication scheme is

used in the synchronization process in [5] and [6]. Consequently, the proposed event-triggered synchronization method can save more network resources than the continuous synchronization methods in [5] and [6].

## VI. CONCLUSION

This article considered the event-triggered  $H_\infty$  synchronization of delayed NNs. A novel integral-based ETS with weighting function of the state of system was proposed to implement the triggering condition. By constructing a novel LKF related to the distributed delay kernel and the weighting function, sufficient conditions for the existence of an event triggered controller that guaranteed the exponential stability with an  $H_\infty$  performance was provided in the form of LMIs. Finally, a numerical example and an application to image encryption had been provided to illustrate the effectiveness of our proposed method.

## REFERENCES

- [1] N. Kumar, B. Singh, and B. K. Panigrahi, "PNKLMF-based neural network control and learning-based HC MPPT technique for multiobjective grid integrated solar PV based distributed generating system," *IEEE Trans. Ind. Informat.*, vol. 15, pp. 3732–3742, Jun. 2019.
- [2] N. Kumar, B. Singh, and B. K. Panigrahi, "LLMLF-based control approach and LPO MPPT technique for improving performance of a multifunctional three-phase two-stage grid integrated PV system," *IEEE Trans. Sustain. Energy*, vol. 11, no. 1, pp. 371–380, Jan. 2019.
- [3] B. Hussain, Q. Du, A. Imran, and M. A. Imran, "Artificial intelligence-powered mobile edge computing-based anomaly detection in cellular networks," *IEEE Trans. Ind. Informat.*, vol. 16, no. 8, pp. 4986–4996, Aug. 2020.
- [4] B. Hu, Z. Guan, N. Xiong, and H. Chao, "Intelligent impulsive synchronization of nonlinear interconnected neural networks for image protection," *IEEE Trans. Ind. Informat.*, vol. 14, no. 8, pp. 3775–3787, Aug. 2018.
- [5] S. Wen, Z. Zeng, T. Huang, Q. Meng, and W. Yao, "Lag synchronization of switched neural networks via neural activation function and applications in image encryption," *IEEE Trans. Neural Netw. Learn. Syst.*, vol. 26, no. 7, pp. 1493–1502, Jul. 2015.
- [6] S. Lakshmanan, M. Prakash, C. P. Lim, R. Rakkiyappan, P. Balasubramanian, and S. Nahavandi, "Synchronization of an inertial neural network with time-varying delays and its application to secure communication," *IEEE Trans. Neural Netw. Learn. Syst.*, vol. 29, no. 1, pp. 195–207, Jan. 2016.
- [7] H. Zhang, Z. Zeng, and Q. L. Han, "Synchronization of multiple reaction-diffusion neural networks with heterogeneous and unbounded time-varying delays," *IEEE Trans. Cybern.*, vol. 99, no. 8, pp. 1–12, Aug. 2018.
- [8] X. M. Zhang, Q. L. Han, X. Ge, and D. Ding, "An overview of recent developments in Lyapunov-Krasovskii functionals and stability criteria for recurrent neural networks with time-varying delays," *Neurocomputing*, vol. 313, pp. 392–401, 2018.
- [9] Q. Song, "Design of controller on synchronization of chaotic neural networks with mixed time-varying delays," *Neurocomputing*, vol. 72, pp. 3288–3295, 2009.
- [10] H. R. Karimi and H. Gao, "New delay-dependent exponential  $H_\infty$  synchronization for uncertain neural networks with mixed time delays," *IEEE Trans. Syst., Man, Cybern., Part B (Cybern.)*, vol. 40, no. 1, pp. 173–185, Feb. 2010.
- [11] X. M. Zhang, Q. L. Han, and B. L. Zhang, "An overview and deep investigation on sampled-data-based event-triggered control and filtering for networked systems," *IEEE Trans. Ind. Informat.*, vol. 13, no. 1, pp. 4–16, Feb. 2017.
- [12] X. M. Zhang and Q. L. Han, "Event-triggered  $H_\infty$  control for a class of nonlinear networked control systems using novel integral inequalities," *Int. J. Robust Nonlinear Control*, vol. 27, pp. 679–700, 2017.
- [13] S. Hu, D. Yue, X. Xie, Y. Ma, and X. Yin, "Stabilization of neural-network-based control systems via event-triggered control with nonperiodic sampled data," *IEEE Trans. Neural Netw. Learn. Syst.*, vol. 29, no. 3, pp. 573–585, Mar. 2018.
- [14] Z. Gu, J. H. Park, D. Yue, Z. G. Wu, and X. Xie, "Event-triggered security output feedback control for networked interconnected systems subject to cyber-attacks," *IEEE Trans. Syst., Man, Cybern.: Syst.*, to be published. doi: 10.1109/TSMC.2019.2960115.
- [15] S. Yan, M. Shen, S. K. Nguang, and G. Zhang, "Event-triggered  $H_\infty$  control of networked control systems with distributed transmission delay," *IEEE Trans. Autom. Control*, to be published. doi: 10.1109/TAC.2019.2953460.
- [16] L. Zhang, H. Gao, and O. Kaynak, "Network-induced constraints in networked control systems—A survey," *IEEE Trans. Ind. Informat.*, vol. 9, no. 1, pp. 403–416, Feb. 2013.
- [17] A. Girard, "Dynamic triggering mechanisms for event-triggered control," *IEEE Trans. Autom. Control*, vol. 60, no. 7, pp. 1992–1997, Jul. 2015.
- [18] P. Tabuada, "Event-triggered real-time scheduling of stabilizing control tasks," *IEEE Trans. Autom. Control*, vol. 52, no. 9, pp. 1680–1685, Sep. 2007.
- [19] D. Yue, E. Tian, and Q. L. Han, "A delay system method for designing event-triggered controllers of networked control systems," *IEEE Trans. Autom. Control*, vol. 58, no. 2, pp. 475–481, Feb. 2012.
- [20] S. Wen, Z. Zeng, M. Chen, and T. Huang, "Synchronization of switched neural networks with communication delays via the event-triggered control," *IEEE Trans. Neural Netw. Learn. Syst.*, vol. 28, no. 10, pp. 2334–2343, Oct. 2017.
- [21] Z. Guo, S. Gong, S. Wen, and T. Huang, "Event-based synchronization control for memristive neural networks with time-varying delay," *IEEE Trans. Cybern.*, vol. 49, no. 9, pp. 3268–3277, Sep. 2019.
- [22] Z. Fei, C. Guan, and H. Gao, "Exponential synchronization of networked chaotic delayed neural network by a hybrid event trigger scheme," *IEEE Trans. Neural Netw. Learn. Syst.*, vol. 29, no. 6, pp. 2558–2567, Jun. 2018.
- [23] S. Ding, Z. Wang, and H. Zhang, "Event-triggered stabilization of neural networks with time-varying switching gains and input saturation," *IEEE Trans. Neural Netw. Learn. Syst.*, vol. 29, no. 10, pp. 5045–5056, Oct. 2018.
- [24] A. Selivanov and E. Fridman, "Event-triggered  $H_\infty$  control: A switching approach," *IEEE Trans. Autom. Control*, vol. 61, no. 10, pp. 3221–3226, Oct. 2016.
- [25] S. H. Mousavi and H. J. Marquez, "Integral-based event triggering controller design for stochastic LTI systems via convex optimisation," *Int. J. Control*, vol. 89, pp. 1416–1427, 2016.
- [26] X. Wang, Z. Fei, H. Gao, and J. Yu, "Integral-based event-triggered fault detection filter design for unmanned surface vehicles," *IEEE Trans. Ind. Informat.*, vol. 15, no. 10, pp. 5626–5636, Oct. 2019.
- [27] H. Alemdar, V. Leroy, A. Prost-Boucle, and F. Petrot, "Ternary neural networks for resource-efficient AI applications," in *Proc. IEEE Int. Joint Conf. Neural Netw.*, Anchorage, AK, USA, 2017, pp. 2547–2554.
- [28] Q. Feng and S. K. Nguang, "Stabilization of uncertain linear distributed delay systems with dissipativity constraints," *Syst. Control Lett.*, vol. 96, pp. 60–71, 2016.
- [29] C. Paleologu, J. Benesty, and S. Ciochina, "A robust variable forgetting factor recursive least-squares algorithm for system identification," *IEEE Signal Process. Lett.*, vol. 15, pp. 597–600, 2008.
- [30] Q. Xia, M. Rao, Y. Ying, and X. Shen, "Adaptive fading Kalman filter with an application," *Automatica*, vol. 30, pp. 1333–1338, 1994.
- [31] B. Singh, N. Kumar, and B. K. Panigrahi, "Steepest descent Laplacian regression based neural network approach for optimal operation of grid supportive solar PV generation," *IEEE Trans. Circuits Syst. II: Express Briefs*, to be published. doi: 10.1109/TCSII.2020.2967106.
- [32] N. Kumar, B. Singh, and B. K. Panigrahi, "Framework of gradient descent least squares regression-based NN structure for power quality improvement in PV-integrated low-voltage weak grid system," *IEEE Trans. Ind. Electron.*, vol. 66, no. 12, pp. 9724–9733, Dec. 2019.
- [33] S. P. Boyd, L. E. Ghaoui, E. Feron, and V. Balakrishnan, *Linear Matrix Inequalities in Systems and Control Theory*. Philadelphia, PA, USA: SIAM, 1994.
- [34] P. Park, J. W. Ko, and C. Jeong, "Reciprocally convex approach to stability of systems with time-varying delays," *Automatica*, vol. 47, pp. 235–238, 2011.
- [35] K. Wang, Z. Teng, and H. Jiang, "Adaptive synchronization of neural networks with time-varying delay and distributed delay," *Physica A: Statistical Mech. Appl.*, vol. 387, pp. 631–642, 2008.
- [36] Y. Wang, L. Xie, and C. E. De Souza, "Robust control of a class of uncertain nonlinear systems," *Syst. Control Lett.*, vol. 19, pp. 139–149, 1992.
- [37] A. Akhavan, A. Samsudin, and A. Akhshani, "A symmetric image encryption scheme based on combination of nonlinear chaotic maps," *J. Franklin Inst.*, vol. 348, pp. 1797–1813, 2011.



**Shen Yan** received the B.E. degree in automation and Ph.D. degree in power engineering automation from the College of Electrical Engineering and Control Science, Nanjing Technology University, Nanjing, China, in 2014 and 2019, respectively.

He is currently a Lecturer with the College of Mechanical and Electronic Engineering, Nanjing Forestry University, Nanjing, China. His current research interests include networked control systems, nonlinear systems, and

event-triggered control.



**Zhou Gu** received the B.S. degree in automation from North China Electric Power University, Beijing, China, in 1997, and the M.S. and Ph.D. degrees in control science and engineering from the Nanjing University of Aeronautics and Astronautics, Nanjing, China, in 2007 and 2010, respectively.

From 1996 to 2013, he was with the School of Power engineering, Nanjing Normal University, Nanjing, China, as an Associate Professor. He was a Visiting Scholar with Central Queensland

University, Rockhampton, QLD, Australia, and The University of Manchester, Manchester, U.K. He is currently a Professor with Nanjing Forestry University, Nanjing, China. His current research interests include networked control systems, time-delay systems, reliable control, and their applications.



**Sing Kiong Nguang** (Senior Member, IEEE) received the B.E. (Hons.) and the Ph.D. degree in electrical and computer engineering from the Department of Electrical and Computer Engineering, University of Newcastle, Callaghan, NSW, Australia, in 1992 and 1995, respectively.

Currently, he is a Chair Professor with the Department of Electrical, Computer and Software Engineering, University of Auckland, Auckland, New Zealand. He has authored or co-authored over 300 refereed journal and conference pa-

pers on nonlinear control design, nonlinear control systems, nonlinear time-delay systems, nonlinear sampled-data systems, biomedical systems modeling, fuzzy modeling and control, biological systems modeling and control, and food and bioproduct processing.

Prof. Nguang has/had served on the editorial board of a number of international journals. He is the Chief-Editor of the *International Journal of Sensors, Wireless Communications and Control*.